Abnormal Posture Detection in an Omni-directional-camera-based Surveillance System

Din-Chang Tseng and Chien-Hung Chen
The Institute of Computer Science and Information Engineering, National Central University, Jhongli, Taiwan
Email: tsengdc@ip.csie.ncu.edu.tw, chienhung66@gmail.com

***Abstract*—In various general environments, the aged or disabled people may fall, squat, or sit down on ground due to sick or dysfunction in move. If the events are unable discovered in time, the fatal danger may be then caused. To reduce the fatal events, an environmental monitoring system for the aged or disabled people is proposed. In this study, four kinds of posture detection are considered in the proposed system: (*i*) fall down and crouch, (*ii*) going out a room without permission, (*iii*) leaving specified area without permission, and (*iv*) recording walk trajectory. An omni-directional camera is used to capture images for monitoring. The background subtraction method is first applied to extract targets. Then principal component analysis (*PCA*) and the change of height of a personal trapezoidal bounding box are used to detect fall down and crouch postures. Several experiments on various environments based on the proposed approach were conducted and evaluated. Stable detection results were obtained to show the feasibility of the proposed system.**

***Index Terms*—surveillance system, abnormal posture detection, omni-directional camera, principal component analysis**

I. Introduction

Automated security surveillance systems need to develop, not only can save money on labor costs, but also for monitoring by the security environment is a major upgrade [1]. General home care monitoring project is mainly divided into two categories: personal behavior and physiological condition monitoring. Although the application is capable of binding to each other, but in achieving both monitoring the use of different techniques. Safety surveillance system research is divided into three parts: a moving object detection, background subtraction and shadow detection. To do surveillance on the environment, we must first be able to capture a moving object in the image sequence.

Temporal difference method [2]-[4], using a continuous image sequences adjacent two images do the subtraction operation, set the threshold to get moving pixels. Background subtraction method [5, 6], using a while to establish the initial background model. Then use the image sequence and the background model to compare new entrants to detect moving pixels. This method can be achieved most complete object pixels, but it is quite sensitive to changes in ambient light, and cannot overcome the problem of camera movement. Optical flow method is using a variation on the estimation of image pixels to infer the position of moving objects. This method can detect when you move the camera still moving object independently, but the disadvantage is fairly complex calculation, if there is no specific hardware, cannot be applied in real-time systems. Background subtraction is quite widely used method of dividing the movement area in the image sequence. The simplest and most common is the use of a background subtraction few seconds of time to build a normal distribution in the background of each pixel, then sent to new imaging sequences and background model for comparison, and set the threshold to distinguish between the foreground and background points many systems take advantage of such a method to detect the movement of the pixel [7]-[14].

Collins *et al*. [15] combined the temporal difference and background subtraction method to detect a moving object. Using the time difference method to detect the moving area, then use in the mobile area background subtraction to obtain complete mobile pixels. Horprasert *et al*. [16] proposed a method to detect moving objects from a static color background images, background model to establish a reference image using a statistical approach. Javed *et al*. [17] proposed a gradient-based background subtraction method, the feature vector from the gradient size and the direction of the composition gradient, based on the establishment of a gradient of the background model. Lu and Tan [18] uses HSV color space to build the background model. Calculate the mean and standard deviation for each pixel location in the image sequence. Use luminance information and chrominance information to distinguish the foreground or background pixels. Haritaoglu *et al*. [19] used a dual mode to detect moving objects in the background, the use of a median filter to distinguish the background pixels moved, and then used static pixels to construct the initial background model, when a moving object within the field of view can still build the background model.

Cucchiara *et al.* [20] detected shadows in *HSV* color space. Because HSV and human perception relatively similar, and can be more accurate in distinguishing shadows. Hu *et al.* [21] proposed the establishment of a conical boundary in the *RGB* color space, used to distinguish shadows, bright light and foreground.

Manuscript received November 24, 2015; revised July 5, 2016.

doi: 10.18178/joace.4.6.397-405

In this paper, we propose a set of personal conduct security surveillance and detection system for monitoring medical environment, providing real-time monitoring personnel to reduce the deterioration. There are four kinds of monitoring in the proposed system: (*i*) fall down and crouch, (*ii*) going out a room without permission, (*iii*) leaving specified area without permission, and (*iv*) recording walk trajectory. We use an omni-directional camera (*omni-camera*) to capture images for monitoring. The camera can easily take 360-degree surround images. In the fall down and crouch detection, we use Principal Component Analysis (*PCA*) to detect the main direction and length of the personal body, and then determine the patient situation. Another method is using the change of the height of the patient trapezoidal bounding box. In the leaving bed detection, we detect whether the patient leaves the pre-defined region or not. However, the criterion tends to result in an unstable judgment; thus we need to check whether the patient really lies flat on the bed. In the leaving ward detection, we first define a linear equation to represent the bottom of a door; if the foot point of a patient is passing through the boundary, the patient is judged leaving ward. In the walking trajectory detection, the foot point of a patient is recorded frame after frame to construct the walking trajectory on the calibrated omni-images.

This paper is structured as follows: In Section II, the discussed omni-camera structure and features that we use. The details of the proposed techniques for use in the system are presented in Sections III–IV. Experimental results are included in Section V, followed by conclusions in Section VI.

II. Structure and Features of Omni-Camera

Many different types of omni-camera, mainly constituted by a CCD photographic lenses and curved mirrors, can be divided into single mirror architecture and double mirror architecture two categories. In this paper, we used is double mirror architecture. Structure and imaging principle and panoramic image conversion method described as follows.

A. Structure and Imaging Principle

Hyperboloidal-shaped in the world coordinates system (WCS), the focal point position respectively (0, 0, c) and (0, 0, -c), as shown in Fig. 1(a). The geometry of the mirror can be described as

$$\frac{X^2+Y^2}{a^2}-\frac{Z^2}{b^2}=-1,\quad c=\sqrt{a^2+b^2} \tag{1}$$

Suppose $Z > 0$ is hyperboloidal-shaped mirror, and the camera is placed in another hyperboloidal-shaped focal point, as shown in Fig. 1(b). O_M expressed as a hyperboloidal- shaped mirror focal position, O_C is the center of the camera's location. Image plane coordinate x, y axes and the world coordinates X、Y axes parallel to each other, and assume that the center position (0, 0, c-f), where f is the focal length of the camera.

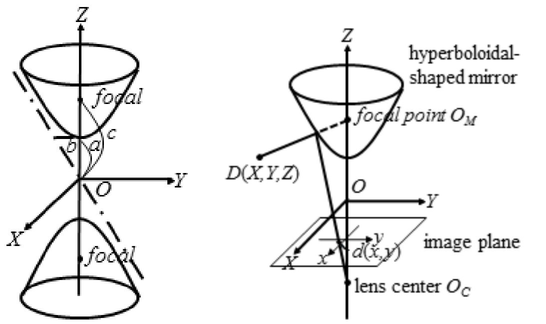

(a) (b)

Figure 1. Camera structure. (a) Hyperboloidal-shaped model. (b) Geometry between hyperboloidal-shaped mirror and camera.

Assuming a point in space $D(X, Y, Z)$ will be reflected by the hyperboloidal-shaped mirror to the camera center O_C, crosses the image plane of the $d(x, y)$, this point is a point in space $D(X, Y, Z)$ of the projection point in the image plane. Feature the relationship between the two points, as shown in Fig. 2. Azimuth angle relationship between the $D(X, Y, Z)$ and $d(x, y)$, as shown in Fig. 2(a). Using the hyperboloidal-shaped longitudinal section projection view, as shown in Fig. 2(b), the geometrical analysis can be deduced relationship equation between the $D(X, Y, Z)$ and $d(x, y)$ as

$$z=\sqrt{X^2+Y^2}\tan\rho+c. \tag{2}$$

$$\rho=\tan^{-1}\frac{(b^2+c^2)\sin\gamma-2bc}{(b^2-c^2)\cos\gamma}. \tag{3}$$

$$\gamma=\tan^{-1}\frac{f}{\sqrt{x^2+y^2}}. \tag{4}$$

where ρ is a $D(X, Y, Z)$ point to the horizontal plane as a reference tilt angle [22], a, b, c is the external parameters of hyperboloidal-shaped mirror, f is focal length of the camera, and γ is the angle between $\overline{dO_c}$ and horizontal plane.

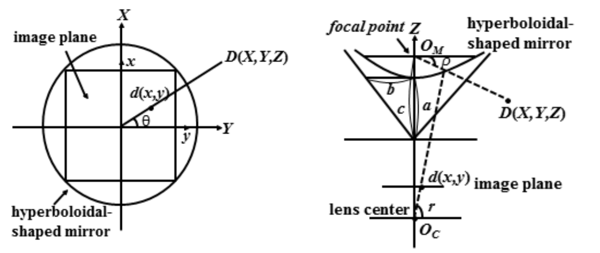

(a) (b)

Figure 2. Feature the relationship between the D(X, Y, Z) and d(x, y). (a) Azimuth angle. (b) Along the Z-axis direction of the hyperboloidal-shaped longitudinal section projection view.

The relationship between the D (X, Y, Z) of a point in space and the projection point $d(x, y)$ in the image plane can be described as

$$\tan(\rho)=\frac{Z-c}{\sqrt{x^2-y^2}}=\frac{(b^2+c^2)\sin r-2bc}{(b^2-c^2)\cos r}=\frac{(b^2-c^2)\tan r-2bc\frac{1}{\cos r}}{(b^2-c^2)}. \tag{5}$$

And we can solve

$$x = \frac{X(b^2 - c^2) f}{(Z-c)(b^2+c^2) - 2bc\sqrt{X^2+Y^2+(Z-c)^2}}. \tag{6}$$

$$y = \frac{Y(b^2 - c^2) f}{(Z-c)(b^2+c^2) - 2bc\sqrt{X^2+Y^2+(Z-c)^2}}. \tag{7}$$

B. Panoramic Image Conversion

Omni-image through hyperboloidal-shaped mirror imaged, so the image will be distorted, and therefore the concept of geometry can be converted through the full range of images into a panoramic image, not only conducive to detect but also image after converted more in line with human viewing mode. Liu *et al.* [23] proposed a fast conversion method. Suppose the point $P(x_1, y_1)$ on the omni-image corresponding to the converted point $p(x, y)$ on the panoramic image, as shown in Fig. 3. Coordinate conversion from omni-image to panoramic image can be described as

$$\rho = \frac{x}{r_1}, r_1 = \frac{r+R}{2}, x_1 = x_0 + (r+y)\sin\rho, y_1 = y_0 + (r+y)\cos\rho. \tag{8}$$

where ρ is the angle between $\overline{OP}$ and *y-axis* in the omni-image, $O(x_0, y_0)$ is the center point of the omni-image, R and r denote the radius of the great circle and the small circle of the omni-image. Only the region between the radius of the great circle and the radius of the small circle was considered to be an effective conversion region. r_1 is the radius of the dotted circle, the dotted circle in the middle of the great circle and the small circle. After the panorama image converted its width is set to the circumferential length of the dotted circle on the omni-image. Then use the interpolation method for performing compression of disc area between the middle circle and great circle on the omni-image, and performing extended action of disc area between the middle circle and the small circle, thus will be able to get a complete rectangle panoramic image.

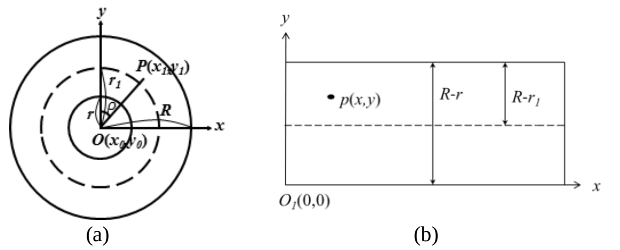

Figure 3. Coordinate conversion from omni-image to panoramic image. (a) Coordinate of the omni-image. (b) Coordinate of the panoramic image.

III. Proposed Techniques for Object Detection

Surveillance system, moving object detection is an important step; this chapter describes motion detection method for motion object, using *PCA* to detect the main direction and length of the personal body, and using the change of the height of the patient trapezoidal bounding box as a benchmark to do detection objects shape methods.

A. Background Subtraction of Motion Detection

The system is divided into four steps of the motion detection. First, select a region of interest (ROI) to be treated, and then build the background model can adapt to changing light or moving objects in the background image, and then use a background subtraction to get moving pixels, and finally on the image to make noise and shadow removal.

1) Select detection area

Although the camera can easily take 360-degree surround images, but because the camera architecture, resulting in images that some regions cannot be observed. For example: central black circular area, peripheral black areas and the ceiling region. To reduce the computational processing time and avoid unnecessary noise generation, so select detection area, as shown in Fig. 4. Only against selected area is processed in the next detection process.

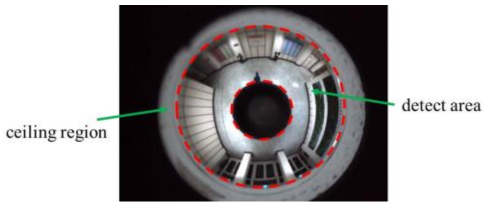

Figure 4. Detect area range.

2) Background gaussian mixture model

Generally used to build the background model is to use a few seconds to establish a Gaussian distribution for each pixel in the background image, this method is to be the background image is the static case. However, in the process of establishing the background, usually encountered as background object to move, whole background image and brightness changes. To solve these problems, this study used a Gaussian mixture model to establish the background image of each pixel and update the background model to adapt to changes in light.

System in the RGB color space to detect moving objects, and use of a few seconds to establish the initial background model. Based on the color information, use of cluster-seeking algorithm)[24] to create a separate K-Gaussian mixture model for each pixel in the background image. Based on (9) probability values can be obtained at each pixel in the background image.

$$P(X) = \sum_{i=1}^{K} \omega_i \eta(X, \mu_i, \mathbf{\Sigma}_i). \tag{9}$$

where K is the number of distribution, ω_i is the weight value at the *i-th* Gaussian mixture model, μ_i is the mean at the *i-th* Gaussian mixture model, $\boldsymbol{\Sigma}_i$ is the covariance matrix at the *i-th* Gaussian mixture model.

The process of establishing the background, the background image may be a moving object or noise generation, which may be a moving object or noise in the background model is built, which may lead to subsequent unable to detect the moving object and the objects of the same color. To solve this problem, First, execute the weight value sorting of each Gaussian mixture model, Taken out front of the *B-th* Gaussian distribution as a background model, as

$$B = \arg\min_{b}\left(\sum_{i=1}^{b} \omega_i > T_{background}\right). \quad (10)$$

where $T_{background}$ is the minimum weight value belongs to the background in the Gaussian mixture model.

Order to adapt the light changes, the background model cannot always remain the same. By changing the background model parameters to achieve adapt to changing light. The mean μ and standard deviation σ, as

$$\mu_t = (1-\alpha)\mu_{t-1} + \alpha X_t. \quad (11)$$

$$\sigma_t^2 = (1-\alpha)\sigma_{t-1}^2 + \sigma(X_t - \mu_t)^T (X_t - \mu_t). \quad (12)$$

where α is the learning rate, $1/\alpha$ is defined as the time constant, expressed distribution parameters change of speed. When the system detects the frame area of the foreground region to achieve the overall 70% or more, detection is stopped, and re-establishing the background, the method as described above.

3) Foreground region detection

After the completion of the initial background model, using the background subtraction the foreground area can be distinguished from the background in each image. Each pixel use background model $B(X)$ to distinguish the pixel of foreground or background. If the pixels x in the image I, that meet one of the background model distribution, as

$$\left|I(x) - \mu_i(x)\right| < \lambda\sigma_i(x). \quad (13)$$

Then this pixel x classified as background point, if pixel x does not comply with the Gaussian distribution of background model, this pixel classified as foreground point. Where μ_i and σ_i denoted as mean and standard deviation at the *i-th* Gaussian distribution.

4) Remove the shadow

According to color theory, shading and background have similar chromaticity values, the difference lies in the shadow of the lower luminance than the background. Use this feature to detect shadows, and will belong to the shaded portion is removed from the foreground area. Assume the vector $c_i = [R_i, G_i, B_i]^T$ and I_i is pixel average value and gray level values at *i-th* Gaussian distribution in background model, and the vector $c_c = [R_c, G_c, B_c]^T$ and I_c denoted as pixel average value and gray level values in the current image. The vector c_c projected to vector c_i, as shown in Fig. 5. Where θ is the angle between two vectors, so we use $\cos\theta$ express the color similarity relations between current color vector c_c and the *i-th* Gaussian distribution color mean vector c_i of the same pixel in background model.

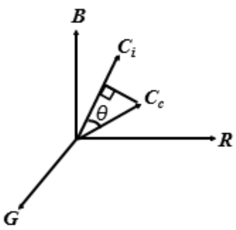

Figure 5. The vector cc projected to vector c_i.

If a pixel accord $\cos\theta > T_{shadow}$, then took the pixels classified as shadows. Remove the shadow of the results, as shown in Fig. 6.

(a) (b) (c)

Figure 6. Remove the shadow. (a) The original image. (b) Foreground area contains shadows. (c) Foreground area after remove the shadow.

B. PCA of Object Orientation Detection

PCA is mainly to find information on the main directions of the most influential and sub-influential, the found these directions orthogonal to each other. Hoping a few directional can represent the variation of the overall data, to reduce the dimensions of the original data.

In order to obtain the orientation of the main axis of the object, so using background subtraction to obtain the foreground area, and records the coordinate position of each pixel in these foreground area, Then use *PCA* to identify the most representative of the distribution of these coordinate points of the first principal component, the first principal component is main axis direction of the object.

C. The Change of the Height of the Patient Trapezoidal Bounding Box as a Benchmark to do Detection Objects Shape

When human behavior changes usually cause the frame to detect the height of the body trapezoidal bounding box followed changes, so use of this feature to achieve the detection of human behavior change. The height of the trapezoidal area is defined as follows:

1) With the omni-image lens center to the outermost point of the effective area of the connection, as the scan line, the positive y-axis is zero degrees, and in a clockwise direction scanning, as shown in Fig. 7.

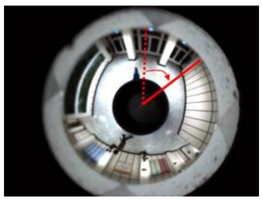

Figure 7. Define the scan line and the scanning direction.

2) Scanned by the foreground area after background subtraction and calculate the distance of these pixels with the center, and only records where the shortest and longest distance from the first through last scan line, as shown in Fig. 8.

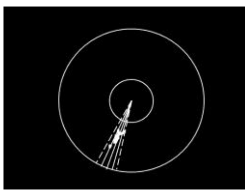

Figure 8. Schematic diagram of the scanning lines intersect the foreground region.

3) Calculate pixels in the first and last one scan line, and center distance equal to its previously recorded the shortest distance, the pixel coordinates of the two points are represented by (x_1, y_1) and (x_2, y_2), and center distance equal to the longest distance, the pixel coordinates of the two points are represented by (x_3, y_3) and (x_4, y_4), then can block out the object of foreground Area, as shown in Fig. 9. And define the start and end coordinates of height of the trapezoid area, as

$$\text{start coordinates equal } \left(\frac{x_1+x_2}{2}, \frac{y_1+y_2}{2}\right). \quad (14)$$

$$\text{end coordinates equal } \left(\frac{x_3+x_4}{2}, \frac{y_3+y_4}{2}\right). \quad (15)$$

Height of the trapezoid area is the distance between start coordinates and end coordinates. Different behaviors have different height, as shown in Fig. 10.

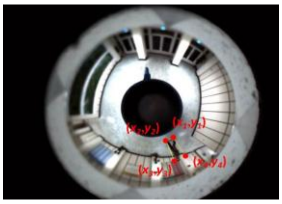

Figure 9. Block out the object of foreground Area.

(a) (b) (c) (d)

Figure 10. Height of the trunk at different behaviors. (a) Normal walking. (b) Fall down. (c) After a fall limbs lump together. (d) Crouch.

IV. Abnormal Posture Detection

Abnormal posture detection focuses on the beds, wards, halls, corridors, outdoor environments. There are four kinds of posture in the proposed system: (*i*) fall down and crouch, (*ii*) going out ward without permission, (*iii*) leaving bed without permission, and (*iv*) recording walk trajectory. These are described in detail below.

A. Patient Fall down and Crouch

When human fall down to occur the height of the trapezoidal are different with normal walking, as shown in Fig. 11. This feature is detected as a basis, so proposed the human foot point on the image to the center point of the detected distance *r* and height of trapezoid area *h* make *r*-*h* curve graph, as shown in Fig. 12. ten asterisk is the obtained experimental data, using the least squares estimation method to fit the curve, because of the different height of the tested officers were obtained *r*-*h* curve will be different, so this curve function is not applicable to all tested officers. When the curves are normalized, the two curves would overlap, so can obtained the different height were obtained *r*-*h* curves has a multiple of the relationship. So can used anyone *r*-*h* function obtained the curve function of human height.

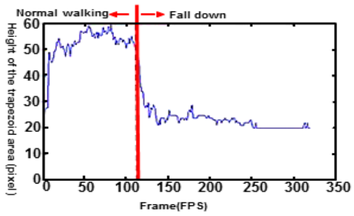

Figure 11. Consecutive images change graph of height of trapezoid area.

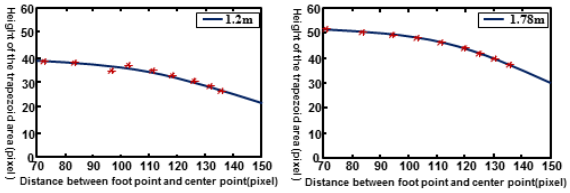

(a) (b)

Figure 12. The different height of the tested officers were obtained r-h curve. (a) 1.2 meter. (b) 1.78 meter.

The *PCA* to detect falls and squat approach, using when a person falls behavior occurs, the body axis direction is different to normal axis direction of walking or standing. But when people to radiation direction of fall or do squat action, simply to the body axis direction method is unable to detect out. So when people to radiation direction of fall or squat, the body axis length will becomes shorter, so as to join the body axis length is another criterion to judge. Using the angle between the two directions and records the maximum and minimum values of the projection to determine whether the falls behavior has occurred or not, as shown in Fig. 13.

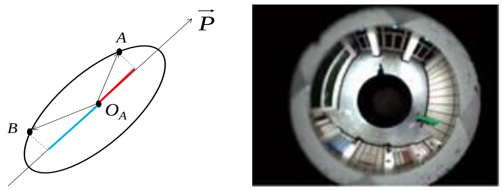

(a) (b)

Figure 13. The main axis length of foreground region. (a) Projection schematic diagram, $\vec{P}$ is the main axis direction, O_A is the average center of foreground region, red line and blue line are denoted as the projected amount in the main axis direction of foreground points A and B. (b) The main axis length in the image (marked with green lines).

B. Going out ward Without Permission

First define the location of the door bottom line, as shown in Fig. 14. Then calculate a linear equation to represent the bottom of a door, and people's feet point, When the foot point through the door bottom line, feet point substituted into linear equation obtained values have positive and negative changes, and the system as the basis for this feature to determine the patient.

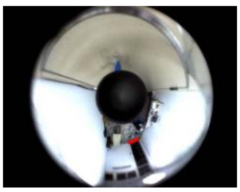

Figure 14. The door bottom line in the image (marked with red lines).

C. Leaving Bed without Permission

First set bed region in the image, as shown in Fig. 15. Then calculate the body average center representative to the location, when the average area of the center falls on the bed, determined whether the person presenting lie flat state or not.

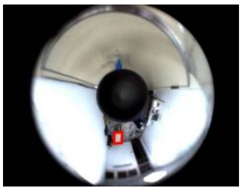

Figure 15. The bed region in the image (marked with red square).

D. Recording Walk Trajectory

1) Lens distortion correction

Omni-camera using the hyperbolic mirror reflected ambient light to the camera for imaging, so the image will be distorted. In order to properly staff walking track record, so it is necessary to perform the full range of image distortion correction. In this using polynomial distortion model to do the lens distortion correction was proposed by Devernay and Faugeras *et al*. [25], the lens distortion model was using infinite series expressed as

$$x_u = x_d(1 + k_1 r_d^2 + k_2 r_d^4 + ...). \quad (16)$$

$$y_u = y_d(1 + k_1 r_d^2 + k_2 r_d^4 + ...). \quad (17)$$

where (x_d, y_d) is distorted image point, (x_u, y_u) is not distorted image point, $r_d = \sqrt{x_d^2 + y_d^2}$ is distance from the distorted image point to image center. Bayer *et al*. [26] proposed the k_1 can be solved to obtain good calibration results. Anti-function model as

$$r_u = r_d(1 + k_1 r_d^2). \quad (18)$$

where $r_u = \sqrt{x_u^2 + y_u^2}$ is distance from the not distorted image point to image center. When get (x_d, y_d) and the corresponding (x_u, y_u), can used least squares estimation method to obtain k_1.

2) Recording walk trajectory

From the full range of image can be observed the foot of the body parts was closest to the camera lens center when a person standing. Therefore, used the pixel whom closest to the camera lens center on the foreground region as a human location point. Then recorded human location point on each image became trajectories image.

V. Experimental Results

In this section, we will show abnormal behavior detection results, including patient fall down and crouch, going out ward and leaving bed without permission, and walking trajectory. System uses capture images device is VS-C14U-80-ST panoramic camera. Experimental videos size is 640 × 480, and capture images rate of 29 frames per second.

A. Patient Fall down and Crouch

In experimental we using the change of the height of the patient trapezoidal bounding box and *PCA* to detect the main direction and length of the personal body method to detection patient fall down and crouch. Experimental videos content included some different posture and directions of fall down and crouched.

The performance of detection method can be addressed by estimating the following parameters: (*i*) True Positive (*TP*) rate, (*ii*) False Negative (*FN*) rate, (*iii*) False Positive (*FP*) rate, and (*iv*) True Negative (*TN*) rate. Then can define the accuracy, sensitivity, and specificity. The following will show detection results in different environments, as shown in Figs. 16 and 17. the mark of red circle is the system detected the fall down or crouch behavior. The detection sensitivity result of two methods detected fall down, as shown in Table I and Table II.

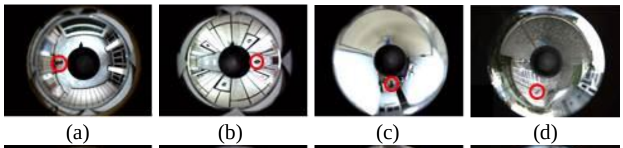

(e) (f) (g) (h)

Figure 16. Patient fall down detection results in different environments of Radiation direction with (a) Hall. (b) Corridor. (c) Ward. (d) Outside. and non-radiation direction with (e) Hall. (f) Corridor. (g) Ward. (h) Outside.

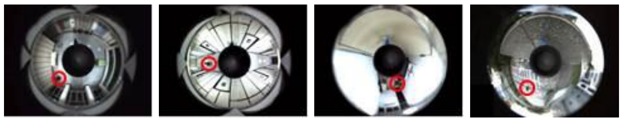

(a) (b) (c) (d)

Figure 17. Crouch behavior detection results in different environments. (a) Hall. (b) Corridor. (c) Ward. (d) Outside.

TABLE I. The Detection Sensitivity Result of the Height of the Patient Trapezoidal Bounding Box Detected Fall Down

Direction of fall	Detected	Not detected	Sensitivity
Radiation direction	12	0	100%
Non-radiation direction	12	0	100%

TABLE II. The Detection Sensitivity Result of the *PCA* to Detect the Main Direction of Fall Down

Direction of fall	Detected	Not detected	Sensitivity
Radiation direction	12	0	100%
Non-radiation direction	12	0	100%

Detection results in different illumination, as shown in Fig. 18. Effectiveness evaluation of two methods to detection results in different illumination as shown in Table III and Table IV. Overall effectiveness evaluation results, as shown in Table V.

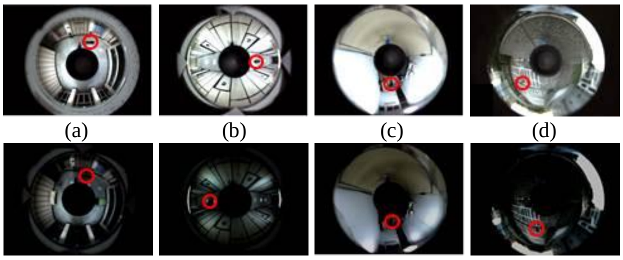

(a) (b) (c) (d) (e) (f) (g) (h)

Figure 18. Fall down detection results in brightness environment with (a) Hall. (b) Corridor. (c) Ward. (d) Outside. and in dark environment with (e) Hall. (f) Corridor. (g) Ward. (h) Outside.

TABLE III. EFFECTIVENESS EVALUATION OF THE HEIGHT OF THE PATIENT TRAPEZOIDAL BOUNDING BOX METHOD TO DETECTION RESULTS IN DIFFERENT ILLUMINATION

Effectiveness evaluation	Brightness	Dark
Accuracy	93%	89%
Precision	92%	82%
Sensitivity	92%	90%
Specificity	94%	88%

TABLE IV. EFFECTIVENESS EVALUATION OF *PCA* METHOD TO DETECTION RESULTS IN DIFFERENT ILLUMINATION

Effectiveness evaluation	Brightness	Dark
Accuracy	89%	80%
Precision	85%	70%
Sensitivity	92%	88%
Specificity	88%	75%

TABLE V. OVERALL EFFECTIVENESS EVALUATION RESULTS OF THE HEIGHT OF THE PATIENT TRAPEZOIDAL BOUNDING BOX AND *PCA* BASE

Effectiveness evaluation	Height of the patient trapezoidal bounding box	*PCA* base
Accuracy	91%	86%
Precision	86%	76%
Sensitivity	92%	93%
Specificity	87%	80%

In Table III and Table IV can observed, in dark environments the detection efficiency of the system is lower than in brightness environments. Because in dark environments, the system detected the foreground region inaccurate, leading to obtain the main axis direction and length and height of the patient trapezoidal bounding box becomes inaccurate. In Table V can observed, the accuracy and sensitivity of the two methods are higher, but in the accuracy, *PCA* base method obtained results is lower.

B. Patient Going out ward without Permission

When the patient through the door area, system will mark the patient location, and determine the patient is entering or going out ward. Continuous images of patient going out ward, as shown in Fig. 19. Overall effectiveness evaluation results, as shown in Table VI.

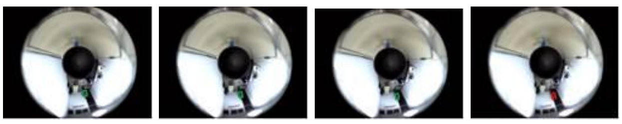

(a) (b) (c) (d)

Figure 19. Continuous images of patient going out ward. (a) - (c) Patient did not through the door area. (d) Patient through the door area and marked out.

TABLE VI. OVERALL EFFECTIVENESS EVALUATION RESULTS OF PATIENT GOING OUT WARD WITHOUT PERMISSION

Effectiveness evaluation	Percent
Accuracy	88%
Precision	83%
Sensitivity	95%
Specificity	81%

C. Patient Leaving Bed without Permission

When detected patient is in the ward, the relationship between the patient and the ward has divided into patient lying on the bed and patient leaving bed these two states. Continuous images of patient leaving bed, as shown in Fig. 20. Overall effectiveness evaluation results, as shown in Table VII.

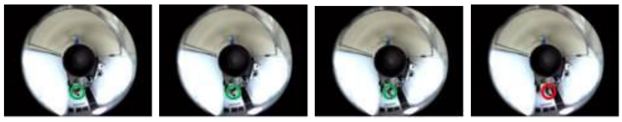

(a) (b) (c) (d)

Figure 20. Continuous images of patient leaving bed. (a) - (c) Patient lying on the bed. (d) Patient leaving bed.

TABLE VII. OVERALL EFFECTIVENESS EVALUATION RESULTS OF PATIENT LEAVING BED WITHOUT PERMISSION

Effectiveness evaluation	Percent
Accuracy	98%
Precision	100%
Sensitivity	95%
Specificity	100%

D. Recording Walk Trajectory

Before to record walk trajectory is necessary to perform the full range of image distortion correction. Corrected image obtained at different values of k_1 as shown in Fig. 21. After completion of the full range of image distortion correction, then can perform the walking trajectory tracking. Recording walk trajectory results as shown in Fig. 22.

(a) (b) (c) (d)

Figure 21. Corrected image obtained at different values of k_1. (a) k_1=0.000020586. (b) k_1=0.000040586. (c) k_1=0.000060586. (d) k_1=0.000080586.

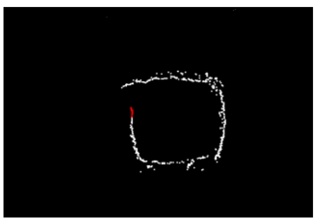

(a)

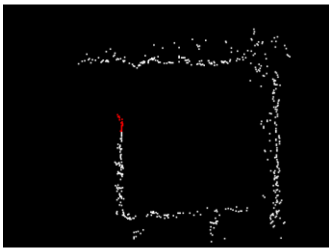

(b)

Figure 22. Walking trajectory tracking results. (a) Not perform distortion correction. (b) After distortion correction.

As in Fig. 22(b), walking trajectory by images after distortion correction is meet the real walking trajectory and direction. When record for some time we can observe the status of activities from staff trajectories, with the degree of trajectory dot density to get staff walking path.

VI. CONCLUSION

In this paper, we use an omni-camera to capture images for monitoring. The camera can easily take 360-degree surround images. We have proposed use *PCA* to detect the main direction and length of the personal body, and another method is using the change of the height of the patient trapezoidal bounding box, and then to determine the patient situation. In experimental, the *PCA* method can perform sixty frames per second, and the height of the patient trapezoidal bounding box method can perform eighty frames per second. The detection rate of the fall down and crouch detection using *PCA* is 93%, and the detection rate of that using the height of the patient trapezoidal bounding box is 92%; the detection rate of leaving bed is 95%; and the detection rate of leaving ward is 95%. The future, system can be added PTZ cameras to increase the detection effectiveness.

REFERENCES

[1] M. Mubashir, L. Shao, and L. Seed, "A survey on fall detection: Principles and approaches," *Neurocomputing*, vol. 100, pp. 144-152, 2013.

[2] W. Hu, T. Tan, L. Wang, and S. Maybank, "A survey on visual surveillance of object motion and behaviors," *IEEE Trans. on Systems, Man, and Cybernetics, Part C:Applications and Reviews*, vol. 34, no. 3, pp. 334-352, 2004.

[3] O. Masoud and P. Papanikolopoulos, "A novel method for tracking and counting pedestrians in real-time using a single camera," *IEEE Trans. on* Vehicular *Technology*, vol. 50, no. 5, pp. 1267-1278, 2001.

[4] Paragios, N. and C. Tziritas, "Detection and location of moving objects using deterministic relaxation algorithms," in *Proc*. *13th Int. Conf. on Pattern Recognition*, Vienna , Austria, Aug.25-29, 1996, pp.201-205.

[5] Fleet, D. J. and A. D. Jepson, "Computation of component image velocity from local phase information," *Int. Journal of Computer Vision*, vol.5, no.1, pp.77-104, 1990.

[6] Wang, M. L., C. C. Huang, and H. Y. Lin, "An intelligent surveillance system based on an omnidirectional vision sensor," in *Proc*. *IEEE Conf. on Cybernetics and Intelligent Systems*, Bangkok, Thailand, Jun.7-9, 2006, pp.1-6.

[7] Lee, D. S., "Effective gaussian mixture learning for video background subtraction," *IEEE Trans. on Pattern Analysis and Machine Intelligence*, vol.27, no.5, pp.827-832, 2005.

[8] Oliver, N. M., B. Rosario, and A. P. Pentland, "A Bayesian computer vision system for modeling human interactions," *IEEE Trans. on Pattern Analysis and Machine Intelligence*, vol.22, no.8, pp.831-843, 2000.

[9] Boult, T. E., R. Micheals, X. Gao, P. Lewis, C. Power, W. Yin, and A. Erkan, "Frame-rate omnidirectional surveillance and tracking of camouflaged and occluded targets," in *Proc*. *2nd IEEE Workshop on Visual Surveillance*, Fort Collins, Colorado, Jul.26, 1999, pp.48-55.

[10] Heikkila, J. and O. Silven, "A real-time system for monitoring of cyclists and pedestrians," in *Proc*. *2nd IEEE Workshop on Visual Surveillance*, Fort Collins, Colorado, Jun.26, 1999, pp.74-81.

[11] Kim, Z., "Real time object tracking based on dynamic feature grouping with background subtraction," in *Proc*. *IEEE Conf. on Conputer Vision and Pattern Recognition*, Anchorage, AK, Jun.23-28, 2008, pp.1-8.

[12] Rehg, J. M., M. Loughlin, and K. Waters, "Vision for a smart kiosk," in *Proc*. *IEEE Conf. on Computer Vision and Pattern Recognition*, San Juan , Puerto Rico, Jun.17-19, 1997, pp.690-696.

[13] Unno, H., K. Ojima, K. Hayashibe, and H. Saji, "Vehicle motion tracking using symmetry of vehicle and background subtraction," in *Proc*. *IEEE Workshop on Vehicles*, Istanbul, Turkey, Jun.13-15, 2007, pp.1127-1131.

[14] Yao, J. and J. M. Odobez, "Multi-layer background subtraction based on color and texture," in *Proc*. *IEEE Conf. on Computer Vision and Pattern Recognition*, Minneapolis, Minnesota, Jun.17-22, 2007, pp.1-8.

[15] Collins, R. T., A. J. Lipton, and T. Kanade, *A System for Video Surveillance and Monitoring*, Technical Report, CMU-RI-TR-00-12, Robotics Institute, Carnegie Mellon University, May 2000.

[16] Horprasert, T., D. Harwood, and L. Davis, "A robust background subtraction and shadow detection," in *Proc*. *Asian Conf. on Computer Vision*, Taipei, Taiwan, Jan.8-11, 2000, pp.983-988.

[17] Javed, O., K. Shafique, and M. Shah, "A hierarchical approach to robust background subtraction using color and gradient information," in *Proc*. *Workshop on Motion and Video Computing*, Orlando, Florida, Dec.5-6, 2003, pp.22-27.

[18] Lu, W. and Y. P. Tan, "A color histogram based people tracking system," in *Proc*. *IEEE Int. Symp. on* Circuits *and Systems*, Sydney, Australia, May 6-9, 2002, pp.137-140.

[19] Haritaoglu, L., D. Harwood, and L. Davis, "W4: real-time surveillance of people and their activities," *IEEE Trans. on Pattern Analysis and Machine Intelligence*, vol.22, no.8, pp.809-830, 2002.

[20] Cucchiara, R. C., C. Grana, G. Neri, M. Piccardi, and A. Prati, "The sakbot system for moving object detection and tracking," in *Video-Based Surveillance Systems:Computer Vision and Distributed Processing*, Kluwer Academic Publishers, Massachusetts, 2001, pp.145-158.

[21] Hu, J. S., T. M. Su, and S. C. Jeng, "Robust background subtraction with shadow and highlight removal for indoor surveillance," in *Proc*. *IEEE Int. Conf. on Intelligent Robots and Systems*, Beijing, China, Oct.9-15, 2006, pp.4545-4550.

[22] Ghidoni, S., A. Pretto, and E. Menegatti, "Cooperative tracking of moving objects and face detection with a dual camera sensor," in *Proc*. *IEEE Int. Conf. on Robotics and Automation*, Padova, Italy, May.3-7, 2010, pp.1050-4729.

[23] Liu, H., W. Pi, and H. Zha, "Motion detection for multiple moving targets by using an omnidirectional camera," in *Proc*. *IEEE Int. Conf. on Robotics, Intelligent Systems and Signal Processing*, Beijing, China, Oct.8-13, 2003, pp.422-426.

[24] Tou, J. T. and R. C. Gonazalez, *Pattern* Recognition *Principles*, Addison-Wesley, Canada, 1974, Ch.3, pp.90-93.

[25] Devernay, F. and O. Faugeras, "Straight lines have to be straight," *Machine Vision and Applications*, vol.13, no.1, pp.14-24, 2001.

[26] Bayer, H. A., "Accurate calibration of CCD camera," in *Proc*. *IEEE Conf. on Computer Vision and Pattern Recognition*, Champaign, IL, Jun.15-18, 1992, pp.96-101.

Din-Chang Tseng received his Ph.D. degree in computer science and information engineering from National Chiao-Tung University, Hsinchu, Taiwan, in June 1988. He has been a professor in the Department of Computer Science and Information Engineering at National Central University, Jhongli, Taiwan since 1996. He is a member of the IEEE. His current research

interests include computer vision, image processing, and virtual reality; especially in the topics of computer vision techniques for advanced driver assistance systems and human computer interaction.

Chien-Hung Chen received his M.S. degree in electrical engineering from National Chung Cheng Institute of Technology, Taoyuan, Taiwan, in 2003. He is currently pursuing the Ph.D. degree in the Department of Computer Science and Information Engineering at National Central University, Jhongli, Taiwan. His research interests include computer vision, image processing, and real-time data processing.